Origin of nematic order in FeSe

Andrey V. Chubukov,[1] Rafael M. Fernandes,[1] and Joerg Schmalian[2]

[1]*School of Physics and Astronomy, University of Minnesota, Minneapolis, Minnesota 55455, USA*

[2]*Institite for Theory of Condensed Matter and Institute for Solid State Physics, Karlsruhe Institute of Technology, 76131 Karlsruhe, Germany*

The origin of the 90-K nematic transition in the chalcogenide FeSe, which displays no magnetic order down to $T = 0$, remains a major puzzle for a unifying theory for the iron-based superconductors. We analyze this problem in light of recent experimental data which reveal very small Fermi pockets in this material. We show that the smallness of the Fermi energy leads to a near degeneracy between magnetic fluctuations and fluctuations in the charge-current density-wave channel. Although the two fluctuation modes cooperate to promote the same preemptive Ising-nematic order, they compete for primary order. We argue that this explains why in FeSe the nematic order emerges when the magnetic correlation length is smaller than in other Fe-based materials. We argue that pressure lifts this near degeneracy and causes nonmonotonic behavior of the nematic transition.

Nematic order in Fe pnictides and Fe chalcogenides develops at a temperature T_s that is larger than the magnetic transition (for reviews, see Ref. [1]). It spontaneously breaks the tetragonal C_4 lattice symmetry down to orthorhombic C_2. The origin of this symmetry breaking is currently one of the most intensely debated issues of the Fe-based superconducting materials [2]. In the Fe pnictides, nematic order occurs reasonably close to the instability towards stripe magnetic order at the Neel temperature T_N. Because the stripe order breaks Z_2 tetragonal symmetry ($C_4 \to C_2$) in addition to the $O(3)$ spin-rotational symmetry and because T_s and T_N show similar doping dependencies, it seems reasonable to associate the nematic order with magnetism [2]. Indeed, several groups have argued [3–12] that magnetic fluctuations split the mean-field stripe magnetic transition into two separate $O(3)$ and Z_2 transitions. The discrete Z_2 symmetry is broken first at $T_s > T_N$, resulting in an intermediate phase, dubbed Ising nematic, where long-range magnetic order is absent but the C_4 lattice symmetry is broken down to C_2. Such Z_2 order triggers orbital and structural order as all three break the same C_4 symmetry.

The magnetic scenario for nematicity in Fe pnictides is supported by a variety of experimental observations, such as the doping dependencies of T_N and T_s [10], the scaling between the shear modulus and the spin-lattice relaxation rate [13], and the sign change in the in-plane resistivity anisotropy between electron-doped and hole-doped Fe pnictides[14]. This scenario, however, has been challenged for the Fe chalcogenide FeSe. This material displays a nematic transition at $T_s \approx 90$ K. The properties of the nematic phase in FeSe resemble those in Fe pnictides: similar softening of the shear modulus [15], similar orthorhombic distortion and orbital order [16–18], and similar behavior of the resistivity anisotropy upon applied strain [19]. Furthermore, a neutron-scattering experiment shows that spin fluctuations are peaked at the same ordering vectors as in the Fe pnictides [20,21]. Yet, in distinction to Fe pnictides, no magnetic order has thus far been observed in FeSe in the absence of external pressure [22,23]. Moreover, NMR measurements were interpreted as evidence that the magnetic correlation length ξ remains small at T_s [15,24]. Although in the Ising-nematic scenario ξ *does not have to be large* at T_s, this seems to be the case for all Fe pnictides.

Given these difficulties with the Ising-nematic scenario, spontaneous orbital order has been invoked to explain the nematic state in FeSe [15,24]. However, at present, no microscopic theory exists where orbital order appears spontaneously instead of being induced by magnetism [25–29]. Alternative scenarios for magnetically driven nematicity in FeSe have also been proposed, involving the formation of a quantum paramagnet [30], the onset of spin quadrupolar order [31], and strong frustration of the magnetic fluctuations [32].

In this Rapid Communication, we present an extension of the spin-nematic scenario which explicitly builds on a unique property of the electronic structure of FeSe, namely, the fact that the Fermi energy E_F in this material is small—only a few meV as seen by angle-resolved photoemission spectroscopy (ARPES) and de Haas–van Alphen experiments [19,33]. For a system with a small E_F, earlier renormalization-group (RG) calculations have shown that there are two density-wave channels whose fluctuations are strong at momenta $(0,\pi)/(\pi,0)$: a spin density-wave (SDW) channel and a charge-current density-wave (CDW) channel (a CDW with an imaginary order parameter, which we denote as iCDW [34]). The relative strength between the two depends on the sign of the interpocket exchange interaction (u_2 in our notations below). For repulsive u_2, the coupling in the SDW channel is larger, whereas for attractive u_2 the coupling in the iCDW channel is larger. In both cases, however, the RG calculations show that the coupling in the subleading channel approaches the one in the leading channel at small energies. The RG process stops at E_F, implying that if E_F is larger than the highest instability temperature (T_s for FeSe) the subleading channel is not a strong competitor and for all practical purposes can be neglected. However, if $E_F \sim T_s$, as in FeSe, the couplings in the two channels become degenerate within the RG. The degeneracy implies that the order parameter manifold increases from $O(3) \times Z_2$ for the three-component SDW or from $Z_2 \times Z_2$ for the one-component iCDW to a larger $O(4) \times Z_2$. In all cases, the Z_2 part of the manifold corresponds to selecting either $(0,\pi)$ or $(\pi,0)$ for the density-wave ordering vector. Although in both $O(3) \times Z_2$ and $O(4) \times Z_2$ models the Z_2 symmetry can be broken before the continuous one, in the latter this happens at a significantly shorter correlation length. As a result, at small E_F, the nematic order emerges while magnetic

fluctuations are still weak. Furthermore, the SDW transition temperature T_N in the $O(4)$ model is additionally suppressed due to the competition with iCDW. We argue that these features explain the properties of the nematic state in FeSe, including nonmonotonic pressure dependence of T_s [35,36].

The model. We consider a quasi-two-dimensional itinerant band model with two hole pockets at the Γ point and two electron pockets at $(0,\pi)$ and $(\pi,0)$ in the 1-Fe Brillouin zone [10,37]. This model can be obtained from an underlying five-orbital model with Hubbard and Hund interactions and hopping between the Fe 3d orbitals [38,39].

The quadratic part of the Hamiltonian in the band basis describes the dispersion of the low-energy fermions, and the information about the orbital content along the Fermi pockets is passed onto interpocket and intrapocket interactions, which are the Hubbard and Hund terms dressed by the matrix elements arising from the change from the orbital to the band basis [40]. The angular dependence of the matrix elements leads to angle-dependent interactions. The three interactions relevant for Ising-nematic order are the interpocket density-density interaction u_1, the exchange interaction u_2, and the pair-hopping interaction u_3 [41]. To simplify the analysis, we follow earlier works [10] and analyze the Ising-nematic order within a RG procedure that: (i) approximates these three interactions as angle independent and (ii) restricts the analysis to one hole pocket. The extension to two pockets and angle-dependent interactions makes the calculations more involved but does not modify the RG equations in any substantial way.

We label the fermions near the hole pocket as $c_{\mathbf{k}}$ and the fermions near the electron pockets as $f_{1,\mathbf{k}}$ and $f_{2,\mathbf{k}}$. The $O(3)$ magnetic order parameter is given by

$$\mathbf{M}_j = \frac{1}{N} \sum_{\mathbf{k}\alpha\beta} (c^\dagger_{\mathbf{k},\alpha} \boldsymbol{\sigma}_{\alpha\beta} f_{j,\mathbf{k}+\mathbf{Q}_j,\beta} + \text{H.c}), \tag{1}$$

whereas the Z_2 iCDW order parameter is

$$\Phi_j = \frac{i}{N} \sum_{\mathbf{k}\alpha} (c^\dagger_{\mathbf{k},\alpha} f_{j,\mathbf{k}+\mathbf{Q}_j,\alpha} - \text{H.c.}), \tag{2}$$

with $j = 1,2$ corresponding to the two possible ordering vectors $\mathbf{Q}_1 = (\pi,0)$ and $\mathbf{Q}_2 = (0,\pi)$. We show the SDW state and a representative of the iCDW state in Fig. 1.

$O(4)$ Ising-nematic action. In the Ising-nematic scenario, the $C_4 \to C_2$ symmetry breaking implies the appearance of a composite order, quadratic in the density-wave order parameters $\mathbf{M}_j$ and Φ_j. To analyze this scenario, we need to know the flow of the couplings that drive SDW order $\Gamma_{\text{sdw}} = u_1 + u_3$ and iCDW order $\Gamma_{\text{icdw}} = u_1 + u_3 - 2u_2$ (Ref. [41]). The bare coupling $\Gamma_{\text{sdw}} > \Gamma_{\text{icdw}}$ when $u_2 > 0$ and $\Gamma_{\text{icdw}} > \Gamma_{\text{sdw}}$ when $u_2 < 0$. As one integrates out the high-energy degrees of freedom via a RG procedure, the ratio $u_2/(u_1 + u_3)$ decreases as the system flows to lower energies (or temperatures) and approaches zero at the energy/temperature scale in which the system develops SDW/iCDW order. This holds, however, only if this scale is larger than E_F. If E_F is larger, the RG flow stops at E_F, and the system develops an instability only in the channel with the largest bare coupling.

To illustrate our point, we plot in Figs. 2(a) and 2(b) the RG flow of Γ_{icdw} and Γ_{sdw} for a particular set of bare couplings $u_1(0) = u_2(0) = 10u_3(0)$, chosen deliberately to
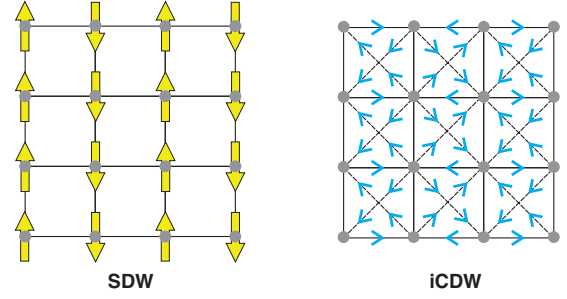

FIG. 1. (Color online) Schematic of the SDW and iCDW ordered states with ordering vector $(\pi,0)$. Although fluctuations in both channels support nematicity, they compete for long-range magnetic and charge orders. For iCDW, one has to distinguish between the pattern of the bond-current order parameter in real space [the real-space version of $i\Phi_i$ from Eq. (2)] and the pattern of the actual current. To obtain the latter, one needs to transform Φ_i to the orbital basis and combine with hoppings. We show the particular current pattern using the same conversion as in Ref. [34]. For $i\Phi_i$ itself, diagonal components are of opposite signs. Other current patterns are also possible as long as they display $(\pi,0)$ order.

give a negative bare Γ_{icdw}. Under the RG flow, Γ_{icdw} becomes positive and approaches Γ_{sdw} at the scale where the couplings diverge and the system develops a density-wave order. The Fermi energy E_F sets the scale at which the RG flow stops. In case I (large E_F), the RG stops when Γ_{icdw} is still small. In case II (smaller E_F), the RG stops when Γ_{icdw} is comparable to Γ_{sdw}, and in case III (even smaller E_F), the RG flow reaches the $O(4)$ fixed point already at energies larger than E_F. We associate case I in Fig. 2 with Fe pnictides, and cases II/III with FeSe based on the values of E_F obtained by ARPES and quantum oscillations [19,33].

We next take the RG results as input and analyze the emergence of a nematic order which spontaneously breaks the symmetry between momenta $\mathbf{Q}_1$ and $\mathbf{Q}_2$ without breaking any other symmetry. The analysis follows the same steps as for pure SDW order [10]: We introduce $\mathbf{M}_j$ and Φ_j ($j = 1,2$) as Hubbard-Stratonovich fields which decouple the four-fermion interaction terms, integrate over the fermions, and obtain the effective action in terms of $\mathbf{M}_j$ and Φ_j,

$$S_{\text{eff}} = \int_{qj} \left(\chi^{-1}_{s,q} \mathbf{M}_j^2 + \chi^{-1}_{c,q} \Phi_j^2 \right) + \frac{u}{2} \int_{xj} \left(\mathbf{M}_j^2 + \Phi_j^2 \right)^2$$

$$- \frac{g}{2} \int_x \left[\left(\mathbf{M}_1^2 + \Phi_1^2 \right) - \left(\mathbf{M}_2^2 + \Phi_2^2 \right) \right]^2, \tag{3}$$

where $\chi^{-1}_{s,q} = \Gamma^{-1}_{\text{sdw}} - \Pi_q$ and $\chi^{-1}_{c,q} = \Gamma^{-1}_{\text{icdw}} - \Pi_q$ with $\Pi_q = \int_k G_{c,k+q} (G_{f_1,k} + G_{f_2,k})$. Note, the only asymmetry between the two order parameters is due to the interactions Γ_{sdw} and Γ_{icdw}, respectively. In particular, we find that in all quartic terms only the $\mathbf{M}_i^2 + \Phi_i^2$ combination appears. Near $\mathbf{Q}_j$, we can expand $\chi^{-1}_{s(c),q} \approx r_{0,s(c)} + \alpha(\mathbf{q} - \mathbf{Q}_j)^2$, where $r_{0,s(c)}$ measures the distance to the SDW (iCDW) mean-field instability and $\alpha \sim O(1)$. The input from the RG analysis is that $r_{0,s}$ and $r_{0,c}$ are close to each other. The quartic coefficients are given by $(u,g) = \pm \frac{1}{2} \int_k G^2_{c,k} (G_{f_1,k} \pm G_{f_2,k})^2$. At $\Gamma_{\text{sdw}} = \Gamma_{\text{icdw}}$, the action depends on $\mathbf{M}$ and Φ only via the combination $\mathbf{M}^2 + \Phi^2$, and the order parameter manifold is $O(4) \times Z_2$.
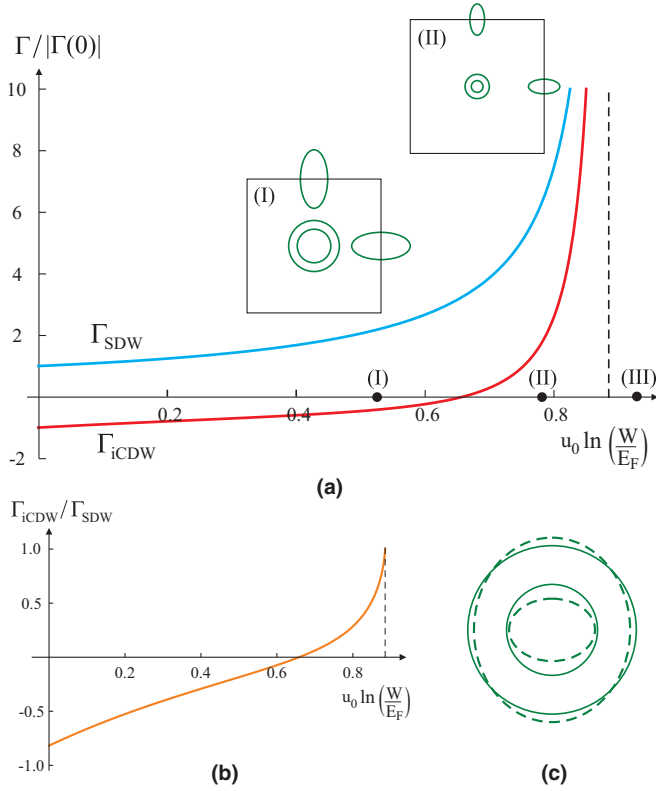
FIG. 2. (Color online) (a) RG flow of the SDW and iCDW interactions Γ_{sdw} (blue curve) and Γ_{icdw} (red curve) as a function of decreasing energy E. W is the bandwidth, $u_0 = u_1(0) = u_2(0) = 10u_3(0)$ is the bare interaction parameter, and the dashed line is the energy in which the two degenerate instabilities occur. The RG flow stops at the Fermi energy E_F: If E_F is large (case I, Fe pnictides), only SDW fluctuations are relevant, whereas if E_F is small (cases II/III, FeSe), both SDW and iCDW fluctuations are important. The insets show schematically the Fermi pockets in each case. (b) Ratio $\Gamma_{\text{icdw}}/\Gamma_{\text{sdw}}$ along the RG flow. (c) Electronic manifestation of the Ising-nematic order on the hole pockets. There is a $\cos 2\theta$ distortion with opposite signs for the two pockets and an overall shift in the chemical potential.

Evaluating the integrals at $E_F \sim T_s$, we find $u > 0$ and $g > 0$, which implies that long-range order selects either $j = 1$ or $j = 2$ but not both, i.e., it breaks both $O(4)$ and Z_2 symmetries.

Within a mean-field approximation, $O(4)$ and Z_2 are broken at the same temperature. Beyond mean field, the Z_2 symmetry is broken first, and *both* $\mathbf{M}$ and Φ contribute to it, even if $\Gamma_{\text{sdw}} \neq \Gamma_{\text{icdw}}$. To see this, we treat $\mathbf{M}$ and Φ as fluctuating fields, introduce the composite fields $\psi = u(\mathbf{M}_1^2 + \Phi_1^2 + \mathbf{M}_2^2 + \Phi_2^2)$ and $\varphi = g(\mathbf{M}_1^2 + \Phi_1^2 - \mathbf{M}_2^2 - \Phi_2^2)$ to decouple the quartic terms, integrate over the primary fields $\mathbf{M}$ and Φ, and obtain the action in terms of ψ and φ,

$$S_{\text{eff}}[\varphi,\psi] = \frac{\varphi^2}{2g} - \frac{\psi^2}{2u} + \frac{3}{2}\int_q \ln\left[\left(\chi_s^{-1} + \psi\right)^2 - \varphi^2\right]$$
$$+ \frac{1}{2}\int_q \ln\left[\left(\chi_c^{-1} + \psi\right)^2 - \varphi^2\right]. \quad (4)$$

The field ψ has a nonzero expectation value $\langle\psi\rangle \neq 0$ at any temperature as it does not break any symmetry but only

renormalizes the correlation lengths of the primary fields $\mathbf{M}$ and Φ to $\xi_{s(c)}^{-2} = r_{0,s(c)} + \langle\psi\rangle$. A nonzero $\langle\varphi\rangle$, on the other hand, breaks the tetragonal C_4 symmetry. If this happens before the susceptibilities of the primary fields soften at $\mathbf{Q}_j$, then the Z_2 rotational symmetry breaks prior to other symmetry breakings. We emphasize that the nematic order parameter φ involves the combination $\mathbf{M}^2 + \Phi^2$, hence one cannot separate SDW-induced and iCDW-induced nematic order, even when χ_s and χ_c are not equivalent.

We solve the action in (4) within the saddle-point approximation, similar to what was performed in Ref. [10]. We find that at $\xi_s, \xi_c \approx \xi$, a nonzero nematic order parameter $\langle\varphi\rangle \neq 0$ emerges when the correlation length is $\xi^2 = \pi/g$ or to logarithmic accuracy in $g \ll 1$ at $T_s = 2\pi\rho_s/|\ln g|$, where ρ_s is the stiffness of the $O(4)$ nonlinear σ model associated with Eq. (3). It is instructive to compare this result with the case where only $O(3)$ SDW fluctuations are present. In that case, the nematic order emerges when $3\xi_{O(3)}^2 = 4\pi/g_{O(3)}$, and the transition temperature is $T_s = 2\pi\rho_s/|\ln\sqrt{g_{O(3)}}|$, where $g_{O(3)}$ is the coupling in the SDW $O(3)$ model. As a result, to obtain the same T_s, one needs a much smaller coupling constant $g_{O(3)} \sim g_{O(4)}^2$. Consequently, at $T = T_s$, the correlation length $\xi_{O(4)}$ in the $O(4)$ case is proportional to $\xi_{O(4)} \sim \sqrt{\xi_{O(3)}}$, i.e., it is much smaller than it would be if nematicity was driven solely by SDW fluctuations. This is consistent with NMR [15,24] and neutron-scattering data [21] in the paramagnetic phase of FeSe, which point to the presence of SDW fluctuations, albeit weaker than in the Fe pnictide compounds. The rapid increase in the correlation lengths below T_s, obeying $\xi_{s,c}^{-2} = \xi_{s,c}^{-2}(T_s) - \langle\varphi\rangle$, is also consistent with the increase in $1/T_1T$ and the inelastic neutron signal [15,21,24].

The $O(4)$ Ising-nematic scenario also addresses why no magnetic order appears down to the lowest temperatures. The SDW and iCDW orders compete via the biquadratic term $(u - g)\mathbf{M}_j^2\Phi_j^2$ in the low-energy action of Eq. (3). As a result, for $u_2 > 0$, fluctuations in the subleading iCDW channel suppress the transition temperature of the leading SDW channel. Such a suppression is the largest when the difference between the coupling constants $|\Gamma_{\text{sdw}} - \Gamma_{\text{icdw}}|$ is the smallest, which happens when the system flows towards $O(4)$ symmetry within the RG, i.e., when E_F is small, such as in FeSe. An alternative approach in which a competing order also suppresses stripe magnetism but favors nematicity was proposed in Ref. [32]. We also note that the smallness of the Fermi pockets in FeSe has been interpreted as an indication that correlations are stronger in these materials than in the pnictides [42]. On the other hand, first-principles calculations seem to correctly predict the value of the specific-heat linear coefficient [33]. Although the issue of how strong the correlations are in FeSe is outside the scope of this Rapid Communication, our RG results should provide in any case a good starting point to analyze the leading instabilities of the system since the material displays well-defined quasiparticles and Fermi pockets as shown by quantum oscillations and ARPES [19].

Experimental signatures. We now discuss the experimental consequences of the Ising-nematic order. The breaking of the Z_2 symmetry between the $j = 1$ and the $j = 2$ components of the $O(4)$ field implies the breaking of the C_4 lattice rotational symmetry down to C_2. This instantaneously triggers structural
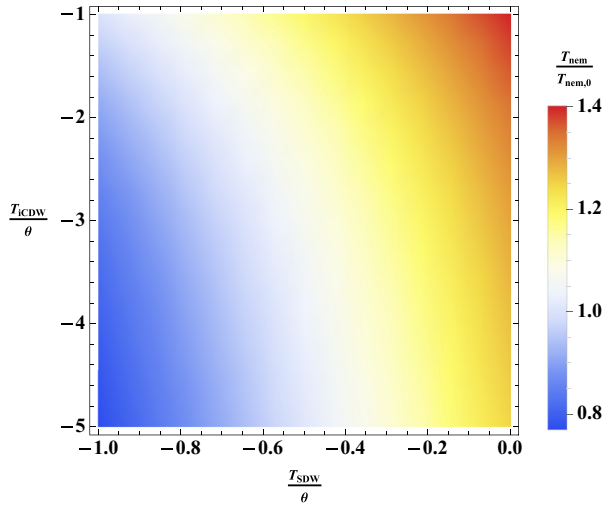
FIG. 3. (Color online) Density plot of the nematic transition T_{nem} as a function of the bare iCDW and SDW transitions T_{iCDW} and T_{SDW}. To mimic the effect of pressure, they start at the same negative value $-\theta$ at zero pressure for which the nematic transition temperature is $T_{\text{nem},0}$ and then vary in opposite ways upon increasing pressure, $T_{\text{iCDW}} < -\theta$ and $T_{\text{SDW}} > -\theta$.

order due to the coupling to the lattice. To investigate how Z_2 order affects the electronic states, we return to the original four-pocket model (with fermions near the two hole pockets described by the operators $c_{1,\mathbf{k}}$ and $c_{2,\mathbf{k}}$) and include the explicit angle dependence introduced by the matrix elements for the transformation between the orbital and the band basis. This transformation has the particularly simple form $c_{1,\mathbf{k}} = d_{xz} \cos \theta_{\mathbf{k}} - d_{yz} \sin \theta_{\mathbf{k}}$, $c_{2,\mathbf{k}} = d_{xz} \sin \theta_{\mathbf{k}} + d_{yz} \cos \theta_{\mathbf{k}}$ if one considers circular hole pockets and neglects the d_{xy} orbital component on the electron pockets [43].

The feedback effect of the Ising-nematic order on the fermions takes place via the self-energy corrections involving the unequal susceptibilities of the primary SDW and iCDW fields at momenta $\mathbf{Q}_1$ and $\mathbf{Q}_2$. These corrections not only shift the chemical potentials of the f_1 and f_2 electron pockets in opposite directions $\langle f_{1,\mathbf{k}}^\dagger f_{1,\mathbf{k}} \rangle - \langle f_{2,\mathbf{k}}^\dagger f_{2,\mathbf{k}} \rangle \propto \langle \varphi \rangle$, but also give rise to a d-wave-like distortion of the c_1 and c_2 hole pockets: $\langle c_{1,\mathbf{k}}^\dagger c_{1,\mathbf{k}} \rangle - \langle c_{2,\mathbf{k}}^\dagger c_{2,\mathbf{k}} \rangle \propto \langle \varphi \rangle \cos 2\theta_{\mathbf{k}}$ [see Fig. 2(b)]. In the orbital basis, the latter corresponds to ferro-orbital order $\langle d_{xz}^\dagger d_{xz} \rangle - \langle d_{yz}^\dagger d_{yz} \rangle \propto \langle \varphi \rangle$ [43]. Proportional to $\langle \varphi \rangle^2$, there is also an overall shift in the chemical potential, symmetric for the two-electron and the two-hole pockets.

The behavior of hole pockets in the Ising-nematic scenario is consistent with the existing ARPES data that show a d-wave-type elongation of one of the hole pockets, whereas the other hole pocket sinks below the Fermi level [19]. The behavior of the electron pockets in the 2-Fe Brillouin zone is also consistent with the splitting of the chemical potentials of the f_1 and f_2 fermions.

We also investigate how pressure affects the nematic transition temperature T_s. Within our approach, T_s is defined by the condition $3\xi_s^2 + \xi_c^2 = 4\pi/g$. Upon pressure, the Fermi pockets become bigger, and the Fermi energy increases. As a result iCDW becomes less competitive, and ξ_c decreases, whereas ξ_s increases. The combination of these two opposite tendencies in general gives rise to a nonmonotonic behavior of T_s. This is illustrated in Fig. 3 using a simple modeling (see the caption).

Note that in our analysis so far we considered $u_2(0) > 0$. If on the other hand this interaction is attractive, $u_2(0) < 0$, the iCDW phase is the leading instability, and the ground-state manifold is $Z_2 \times Z_2$. In this case, the nematic and iCDW transitions are expected to be simultaneous [10]. Although at present no microscopic mechanism is known to give $u_2(0) < 0$ [34], this could be another possibility to explain the existence of nematic order without magnetic order in FeSe. Note also that the near degeneracy between SDW and iCDW gives rise to nucleation of the local iCDW order in the presence of pointlike impurities, which favor iCDW against SDW [44].

Summary. To summarize, we propose a natural extension of the Ising-nematic scenario to explain the puzzling nematic state observed in FeSe. Our scenario relies on the smallness of E_F and explains the onset of nematic order far from magnetism due to the near degeneracy between the SDW channel and an iCDW charge-current density-wave channel. Although these fluctuations cooperate with magnetic ones to break the tetragonal symmetry, they compete for long-range order and reduce both the T_N and the magnetic correlation length at the onset of nematic order. We argue that this Ising-nematic scenario can also explain the observed nonmonotonic dependence of the nematic transition temperature T_s upon pressure.

[1] D. C. Johnston, Adv. Phys. **59**, 803 (2010); D. N. Basov and A. V. Chubukov, Nat. Phys. **7**, 272 (2011); J. Paglione and R. L. Greene, *ibid.* **6**, 645 (2010); P. C. Canfield and S. L. Bud'ko, Annu. Rev. Condens. Matter Phys. **1**, 27 (2010); H. H. Wen and S. Li, *ibid.* **2**, 121 (2011); P. Dai, J. Hu, and E. Dagotto, Nat. Phys. **8**, 709 (2012).

[2] R. M. Fernandes, A. V. Chubukov, and J. Schmalian, Nat. Phys. **10**, 97 (2014).

[3] C. Xu, M. Müller, and S. Sachdev, Phys. Rev. B **78**, 020501(R) (2008).

[4] C. Fang, H. Yao, W.-F. Tsai, J. P. Hu, and S. A. Kivelson, Phys. Rev. B **77**, 224509 (2008).

[5] E. Abrahams and Q. Si, J. Phys.: Condens. Matter **23**, 223201 (2011).

[6] I. I. Mazin and M. D. Johannes, Nat. Phys. **5**, 141 (2009).

[7] Y. Kamiya, N. Kawashima, and C. D. Batista, Phys. Rev. B **84**, 214429 (2011).

[8] M. Capati, M. Grilli, and J. Lorenzana, Phys. Rev. B **84**, 214520 (2011).

[9] P. M. R. Brydon, J. Schmiedt, and C. Timm, Phys. Rev. B **84**, 214510 (2011).

[10] R. M. Fernandes, A. V. Chubukov, J. Knolle, I. Eremin, and J. Schmalian, Phys. Rev. B **85**, 024534 (2012).

[11] S. Liang, A. Moreo, and E. Dagotto, Phys. Rev. Lett. **111**, 047004 (2013).

[12] H. Yamase and R. Zeyher, arXiv:1503.07646.

[13] R. M. Fernandes, A. E. Böhmer, C. Meingast, and J. Schmalian, Phys. Rev. Lett. **111**, 137001 (2013).

[14] E. C. Blomberg, M. A. Tanatar, R. M. Fernandes, I. I. Mazin, B. Shen, H.-H. Wen, M. D. Johannes, J. Schmalian, and R. Prozorov, Nat. Commun. **4**, 1914 (2013).

[15] A. E. Böhmer, T. Arai, F. Hardy, T. Hattori, T. Iye, T. Wolf, H. v. Löhneysen, K. Ishida, and C. Meingast, Phys. Rev. Lett. **114**, 027001 (2015).

[16] K. Nakayama, Y. Miyata, G. N. Phan, T. Sato, Y. Tanabe, T. Urata, K. Tanigaki, and T. Takahashi, Phys. Rev. Lett. **113**, 237001 (2014).

[17] P. Zhang, T. Qian, P. Richard, X. P. Wang, H. Miao, B. Q. Lv, B. B. Fu, T. Wolf, C. Meingast, X. X. Wu, Z. Q. Wang, J. P. Hu, and H. Ding, arXiv:1503.01390.

[18] Y. Zhang, M. Yi, Z.-K. Liu, W. Li, J. J. Lee, R. G. Moore, M. Hashimoto, N. Masamichi, H. Eisaki, S.-K. Mo, Z. Hussain, T. P. Devereaux, Z.-X. Shen, and D. H. Lu, arXiv:1503.01556.

[19] M. D. Watson, T. K. Kim, A. A. Haghighirad, N. R. Davies, A. McCollam, A. Narayanan, S. F. Blake, Y. L. Chen, S. Ghannadzadeh, A. J. Schofield, M. Hoesch, C. Meingast, T. Wolf, and A. I. Coldea, Phys. Rev. B **91**, 155106 (2015).

[20] M. C. Rahn, R. A. Ewings, S. J. Sedlmaier, S. J. Clarke, and A. T. Boothroyd, Phys. Rev. B **91**, 180501(R) (2015).

[21] Q. Wang, Y. Shen, B. Pan, Y. Hao, M. Ma, F. Zhou, P. Steffens, K. Schmalzl, T. R. Forrest, M. Abdel-Hafiez, D. A. Chareev, A. N. Vasiliev, P. Bourges, Y. Sidis, H. Cao, and J. Zhao, arXiv:1502.07544.

[22] T. M. McQueen, A. J. Williams, P. W. Stephens, J. Tao, Y. Zhu, V. Ksenofontov, F. Casper, C. Felser, and R. J. Cava, Phys. Rev. Lett. **103**, 057002 (2009).

[23] T. Imai, K. Ahilan, F. L. Ning, T. M. McQueen, and R. J. Cava, Phys. Rev. Lett. **102**, 177005 (2009).

[24] S.-H. Baek, D. V. Efremov, J. M. Ok, J. S. Kim, J. van den Brink, and B. Büchner, Nature Mater. **14**, 210 (2014).

[25] C. C. Lee, W. G. Yin, and W. Ku, Phys. Rev. Lett. **103**, 267001 (2009).

[26] C.-C. Chen, J. Maciejko, A. P. Sorini, B. Moritz, R. R. P. Singh, and T. P. Devereaux, Phys. Rev. B **82**, 100504 (2010).

[27] W. Lv, F. Krüger, and P. Phillips, Phys. Rev. B **82**, 045125 (2010).

[28] W.-C. Lee and P. W. Phillips, Phys. Rev. B **86**, 245113 (2012).

[29] S. Onari and H. Kontani, Phys. Rev. Lett. **109**, 137001 (2012).

[30] F. Wang, S. Kivelson, and D.-H. Lee, arXiv:1501.00844.

[31] R. Yu and Q. Si, arXiv:1501.05926.

[32] J. K. Glasbrenner, I. I. Mazin, H. O. Jeschke, P. J. Hirschfeld, and R. Valenti, arXiv:1501.04946.

[33] T. Terashima *et al.*, Phys. Rev. B **90**, 144517 (2014).

[34] J. Kang and Z. Tesanovic, Phys. Rev. B **83**, 020505 (2011).

[35] M. Bendele, A. Ichsanow, Y. Pashkevich, L. Keller, T. Strassle, A. Gusev, E. Pomjakushina, K. Conder, R. Khasanov, and H. Keller, Phys. Rev. B **85**, 064517 (2012).

[36] T. Terashima, N. Kikugawa, S. Kasahara, T. Watashige, T. Shibauchi, Y. Matsuda, T. Wolf, A. E. Böhmer, F. Hardy, C. Meingast, H. v. Löhneysen, and S. Uji, J. Phys. Soc. Jpn. **84**, 063701 (2015).

[37] I. Eremin and A. V. Chubukov, Phys. Rev. B **81**, 024511 (2010).

[38] S. Graser, T. A. Maier, P. J. Hirschfeld, and D. J. Scalapino, New J. Phys. **11**, 025016 (2009).

[39] The low-energy excitations in the band basis come from three orbitals—d_{xz}, d_{yz}, and d_{xy}. The two hole pockets are composed predominantly of d_{xz} and d_{yz} orbitals, and the two electron pockets of d_{xy} and d_{xz} orbitals [$(0,\pi)$ pocket] or d_{xy} and d_{yz} orbitals [$(\pi,0)$ pocket].

[40] L. Fanfarillo, A. Cortijo, and B. Valenzuela, arXiv:1410.8488.

[41] A. V. Chubukov, D. V. Efremov, and I. Eremin, Phys. Rev. B **78**, 134512 (2008); A. V. Chubukov, Physica C **469**, 640 (2009); S. Maiti and A. V. Chubukov, Phys. Rev. B **82**, 214515 (2010).

[42] M. Aichhorn, S. Biermann, T. Miyake, A. Georges, and M. Imada, Phys. Rev. B **82**, 064504 (2010).

[43] R. M. Fernandes and O. Vafek, Phys. Rev. B **90**, 214514 (2014); V. Cvetkovic and O. Vafek, *ibid.* **88**, 134510 (2013).

[44] M. Hoyer, M. S. Scheurer, S. V. Syzranov, and J. Schmalian, Phys. Rev. B **91**, 054501 (2015).